Research Article

Efficient numerical schemes on modified graded mesh for singularly perturbed parabolic convection-diffusion problems

K.K. Sah*,

Abstract

In this study, numerical approaches to the singularly perturbed problems of convection diffusion type are presented. The backward Euler method is applied to a uniform mesh in the temporal domain, while in the spatial domain, we utilize both the hybrid midpoint finite difference scheme and the high order via differential identity expansion scheme on a modified graded mesh. The solution to the problem introduces a boundary layer on the right side of the domain. Both of the above methods are proven to have identical convergence with respect to the perturbation parameter. We also provide numerical results in order to verify the theoretical conclusions. We demonstrate that the applied approaches provide uniform convergence of first-order in the temporal variable and second-order up to a logarithmic factor with respect to the spatial variable.

AMS subject classifications (2020): 65M06, 65M12, 65M15.

*Corresponding author

Received 14 May 2025; revised 3 August 2025; accepted 14 August 2025

Kishun Kumar Sah

Department of Mathematics, National Institute of Technology Patna, India.

e-mail: kishuns.phd20.ma@nitp.ac.in

Keywords: Perturbation problems; Uniform convergence; Modified graded mesh, Boundary layers; Hybrid midpoint finite difference scheme; HODIE finite difference scheme

1 Introduction and summary

A singular perturbation problem in the context of parabolic partial differential equations involves a small parameter (usually denoted by ε) multiplying the highest-order time derivative term in the equation. One example of a singular perturbation problem is the parabolic convection-diffusion equation, which models the transport of a scalar quantity, such as heat or chemical concentration, in a fluid medium that is subject to both diffusion and convection. The equation takes the form: $\varepsilon u_t = D u_{xx} - v u_x$, where $u(x,t)$ is the scalar quantity being transported and ε is the small parameter that measures the relative strength of diffusion to convection. This equation is called the parabolic convection-diffusion equation because it is a parabolic partial differential equation that combines convection and diffusion terms. The convection term $v u_x$ represents the transport of the scalar quantity by the fluid flow, while the diffusion term $D u_{xx}$ represents the spreading of the scalar quantity due to molecular diffusion. The singular perturbation aspect of this problem arises because the εu_t term introduces a time scale that is much faster than the time scale of the diffusion and convection terms. As a result, the solution to this equation exhibits behavior that is very different depending on whether ε is small or not. These problems frequently occur in a variety of applied mathematics fields, including fluid dynamics, elasticity, and many others. The study of singular perturbation problems like the parabolic convection-diffusion equation is important in many fields, including fluid dynamics, chemical engineering, and mathematical biology. Techniques for analyzing these problems include matched asymptotic expansions, boundary layer theory, and numerical methods that accurately depict the solution's behavior as the parameter ε tends towards zero. When the value of ε is small, the problem exhibits heightened sensitivity to alterations in initial or boundary conditions, rendering conventional numerical methods for solving parabolic equations seemingly insufficient and imprecise.

Addressing singular perturbation problems necessitates the application of specialized techniques like asymptotic analysis, matched asymptotic expansions, or numerical methods explicitly tailored for these specific types of problems. The goal is to accurately capture the behavior of the solution in the boundary layer regions while avoiding excessive computational cost or numerical instability. Approximate solutions are required in these situations since it is often impossible or very difficult to find the precise answer to these mathematical issues. By using perturbation techniques, it is possible to find a rough answer. These approaches fundamental premise is to start by finding a solution to a reduced problem and thereafter get consistently excellent estimates. The solution of the singular perturbation in the parabolic partial differential equations relies on both the resolution at the previous stage and the resolution at the present stage; it is more analogous to events that occur in the actual world. Many publications addressing singularly perturbed parabolic problems are accessible in the literature.

For instance, Claver, Gracia, and Jorge [3] developed high-order numerical methods for one-dimensional parabolic singularly perturbed problems, providing valuable insights into handling regular and singular layers. Clavero, Gracia, and Lisbona [5] extended these methods by implementing higher-order schemes on Shishkin meshes for convection-diffusion problems, ensuring uniform convergence. Izadi and Yuzbasi [8] proposed a hybrid approximation scheme that effectively tackled convection-diffusion problems with singular perturbations. Mukherjee and Natesan [17] introduced parameter-uniform hybrid schemes for convection-dominated initial-boundary-value problems, while their subsequent work [18] employed Richardson extrapolation techniques to enhance solution accuracy and robustness. Furthermore, Tia, Liu, and An [22] devised a higher-order finite difference scheme for singularly perturbed parabolic problems, emphasizing improved computational efficiency.

Despite these advancements, analytical solutions to singularly perturbed differential equations remain challenging due to the inherent complexity of boundary and interior layers.

Furthermore, the problem of the solution displays border and interior layers with a modest perturbation parameter of ε. Also, on a uniform mesh, the classical numerical technique suddenly needs a lot of mesh points to correctly

represent the layer in the solution, which is not feasible. In this sense, the aforementioned approach is unsuccessful. So, a uniform convergent approach has been developed as a result of the specific consideration needed for the numerical solution of singularly perturbed partial differential equations.

There are numerous studies focused on the analytical and numerical treatment of singularly perturbed parabolic problems, particularly utilizing finite difference and finite element methods. For instance, Cai and Liu [1] proposed a Reynolds-uniform scheme for addressing such problems, emphasizing uniform convergence. Chi-kuang [2] applied finite element methods to tackle singular perturbation problems, showcasing their versatility in handling boundary layers. Moreover, Clavero, Jorge, and Lisbona [4] developed uniformly convergent schemes that integrated alternating directions and exponential fitting techniques, enhancing solution accuracy. Kadalbajoo and Yadaw [9] investigated parameter-uniform finite element methods for two-parameter problems, extending their applicability to reaction-diffusion systems. Additionally, Kumar and Vigo-Aguiar [15] devised a parameter-uniform grid equidistribution method, offering improved robustness in degenerate parabolic problems. Sun and stynes [21] employed finite element methods for high-order elliptic singularly perturbed problems. However, analytical solutions and numerical approaches for singular perturbation convection diffusion problems are only briefly explored in a few papers. Mukherjee and Natesan [17] proposed hybrid numerical schemes that maintain uniform convergence in convection-diffusion settings. Vulanović and Nhan [24] advanced this by developing robust higher-order hybrid schemes, which effectively handle steep gradients. Similarly, the higher-order monotone schemes designed by Vulanović [23] demonstrate significant accuracy in nonlinear singular perturbation problems. In terms of the diffusion parameter, the numerical technique is uniformly convergent, with an order close to two in space, but in all these works, the authors have described a singularly perturbed parabolic problem on a Shishkin mesh only.

There are currently no known papers relating to the convergence of difference schemes on modified graded meshes. As a result, we are now in a position to develop a different scheme for a modified graded mesh. Motivated by the work of Claver, Gracia, and Jorge [3], who developed high-

order numerical methods for singularly perturbed problems on layer-adapted meshes, Kaushik et al. [10], who introduced a modified graded mesh for singularly perturbed reaction-diffusion problems, achieving enhanced accuracy, Mukherjee and Natesan [18], who demonstrated robust convergence for convection-diffusion problems by using the Richardson extrapolation technique, Clavero, Gracia, and Stynes [6], who provided a simplified analysis of hybrid numerical methods, and Kaushik et al. [11], who applied higher-order methods to two-parameter singular perturbation problems, we aim to extend this research direction.

In this article, we propose two finite difference schemes: the hybrid midpoint finite difference scheme and the high order via differential identity expansion (HODIE) finite difference scheme on a modified graded mesh for the convection-diffusion parabolic problem. Consider the singularly perturbed initial-boundary value problem:

$$
\begin{cases}
\dfrac{\partial y(r,\theta)}{\partial \theta} + \mathscr{L}_\varepsilon y = f(r,\theta) & \text{on } \Lambda := \Lambda_r \times \Lambda_\theta, \\
& \text{where } \Lambda_r = (0,1) \text{ and } \Lambda_\theta = (0,\mathscr{T}], \\
y(r,0) = y_0(r) & \text{for } 0 \le r \le 1, \\
y(0,\theta) = 0 & \text{for } 0 < \theta \le \mathscr{T}, \\
y(1,\theta) = 0 & \text{for } 0 < \theta \le \mathscr{T},
\end{cases}
\tag{1}
$$

where

$$
\mathscr{L}_\varepsilon y(r,\theta) \equiv -\varepsilon \frac{\partial^2 y(r,\theta)}{\partial r^2} + \kappa_1(r)\frac{\partial y(r,\theta)}{\partial r} + \kappa_2(r,\theta)y(r,\theta),
\tag{2}
$$

with $\kappa_1(r) > \lambda > 0$ and $\kappa_2 = \kappa_2(r,\theta) \ge 0$ on $\overline{\Lambda}$, where ε is a small perturbation. In section 2, there will be more presumptions made regarding the problem of the data. From (8), it can be found that the solution y of (1) contains an exponential boundary layer at the side $r = 1$ of Λ. Throughout this paper, we concentrate on two finite difference techniques (hybrid difference scheme and second-order HODIE) for (1) that were introduced and examined in [3, 17]. These studies verify convergence for these approaches, uniformly in ε, with the caveat that $\kappa_2 = \kappa_2(r)$, but the mesh is the same in both papers.

Our main goal in this study is to suggest and examine a higher-order hybrid finite difference strategy for the problem (1) on the modified graded mesh, which shall be discussed in the forthcoming section. In Section 3, we define the meshes for temporal and spatial discretization and introduce some special difference operators and the finite difference scheme. Also, we will prove that the methods finite difference techniques (hybrid difference scheme and second-order HODIE) of [3, 17] are essentially the same. In Section 4, we show the convergence of these numerical techniques, uniformly in ε when applied to (1). In Section 5, we present the numerical results for two linear test problems to validate the theoretical results. Finally, in Section 6, we summarize the main conclusions.

The functions based on the mesh assumption (16), which proves to be considerably less limiting compared to the mesh constraint $\mathscr{N}^{-k} \leq \mathscr{C}\Delta\theta$ imposed in [3, 17], where $k \in (0,1)$. When $\varepsilon \leq \mathscr{N}^{-1}$, our convergence result Theorem 1 becomes

$$\max_{i,j} \left| y(r_i, \theta_j) - Y_i^j \right| \leq \mathscr{C}[\Delta\theta + (\mathscr{N}^{-1}\ln(1/\varepsilon))^2]. \qquad (3)$$

This sharpens the weaker result

$$\max_{i,j} \left| y(r_i, \theta_j) - Y_i^j \right| \leq \mathscr{C}[\Delta\theta + \mathscr{N}^{-2+k}(\ln 1/\varepsilon)^2].$$

It was obtained from [3, 17]. The numerical findings shown in these papers demonstrate that the factor $\mathscr{N}^k$ in this instance is an antiquity of the analysis; that is, that our bound (3) is sharp. In section 5, we provide yet another numerical example to demonstrate the accuracy of our convergence results. In section 6, some final conclusions are given.

Notation: Throughout the paper, the symbol $\mathscr{C}$ represents a general positive constant that remains unaffected by both ε and the mesh size.

2 Assumptions on the data

Before we analyze the problem, some of the compatibility conditions are necessary. Therefore, the following compatibility conditions at the corners

for functions and their zero-order and first-order derivatives are assumed to satisfy:

$$
\begin{cases}
y_0(0) = y_0(1) = 0, \\
-\varepsilon y_0^{''}(0) + \kappa_1(0)y_0^{'}(0) = f(0,0), \\
-\varepsilon y_0^{''}(1) + \kappa_1(1)y_0^{'}(1) = f(1,0).
\end{cases}
\tag{4}
$$

Then (1) has a unique solution in the Holder space $\mathscr{C}^{2+\lambda,1+\lambda/2}(\overline{\Lambda})$ see in [19, 7]. We also make the assumption that the corner compatibility conditions of second order are met, ensuring the validity of $\mathscr{C}^{4+\lambda,2+\lambda/2}(\overline{\Lambda})$. These conditions can be explicitly stated within the terms of the problem of data in the following manner. Differentiating (1) with respect to θ we get

$$
f_\theta = y_{\theta\theta} + \mathscr{L}_\varepsilon y_\theta + \kappa_{2\theta}y = y_{\theta\theta} + \mathscr{L}_\varepsilon(f - \mathscr{L}_\varepsilon y) + \kappa_{2\theta}y.
$$

Therefore, by invoking (1) and (4), we can express the second-order corner compatibility conditions as

$$
\mathscr{L}_\varepsilon(\mathscr{L}_\varepsilon y_0) = \mathscr{L}_\varepsilon f - f_\theta
\tag{5}
$$

at the corners $(0,0)$ and $(1,0)$. Given these assumptions, the solution y to (1) exhibits an exponential layer along the boundary $r = 1$ of Λ and adheres to the specified bound

$$
\left| \frac{\partial^{s+l}y(r,\theta)}{\partial r^s \partial \theta^l} \right| \leq \mathscr{C}(1 + \varepsilon^{-s}e^{-\lambda(1-r)/\varepsilon}) \quad for \quad (r,\theta) \in \overline{\Lambda} \quad and \quad s + 2l \leq 4.
\tag{6}
$$

This result was proved in [25] for $0 \leq s+l \leq 2$. Under necessary compatibility conditions and sufficient smoothness on the data, the proof of the estimate (6) for higher values of s, l follows similarly from [3, Lemma 2.1]. The approaches given in [19] may be used to prove the aforementioned bound. The inequality (6) a priori is sufficient for the majority of our analysis. It becomes necessary for us to additionally assume that the data of the problem (1) adhere to the third-order compatibility condition

$$
f_{\theta\theta} = \mathscr{L}_\varepsilon(f_\theta - \mathscr{L}_\varepsilon(f - \mathscr{L}_\varepsilon y_0) - \kappa_{2\theta}y_0) \text{ at the corners } (0,0) \text{ and } (1,0).
\tag{7}
$$

Then, similarly to (6), the bounds on the derivatives can be shown as

$$\left| \frac{\partial^{s+l} y(r,\theta)}{\partial r^s \partial \theta^l} \right| \leq \mathscr{C}(1 + \varepsilon^{-s} e^{-\lambda(1-r)/\varepsilon}) \ \text{ for } (r,\theta) \in \overline{\Lambda} \text{ and } s + 2l \leq 6. \quad (8)$$

In [3, 17], authors assumed that (8) is valid for $s + l \leq 4, \ \ l \leq 2$.

Remark 1. The order of convergence of the our numerical technique on a modified graded mesh, applied the finite difference scheme(midpoint technique), and the HODIE finite difference scheme is unaffected when (7) is broken, according to the findings of our calculations. For an illustration, see section 5.

Remark 2. As the variable ε can assume a range of values, the compatibility condition (4) indicates that

$$\begin{cases} y_0(0) = y_0(1) = 0, \\ \kappa_1(0) y_0^{'}(0) = f(0,0), \\ \kappa_1(1) y_0^{'}(1) = f(1,0), \\ y_0^{''}(0) = y_0^{''}(1) = 0. \end{cases} \quad (9)$$

Likewise, by utilizing (9), it becomes apparent that the equivalence of (5) is contingent upon the condition of requiring.

$$\begin{cases} (\kappa_1^{'} + \kappa_2) f = \kappa_1 f_r - f_\theta, \\ (\kappa_1^{''} + 2\kappa_{2r}) y_0^{'} = f_{rr}, \\ y_0^4 = 0 \end{cases}$$

at the corners $(0,0)$ and $(1,0)$.

Further requirements are imposed on the data by assumption (7), although as Remark 1 shows, they may not be necessary in reality. Despite the fact that these requirements place limits on the types of data that are allowed, it is nonetheless evident that some types of data meet these requirements. For instance, if enough derivatives of the y_0 and f disappear at the corners $(0,0)$ and $(1,0)$.

3 Numerical discretization

Grids for spatial and temporal direction and bounds on them are defined in this section. We apply two finite difference schemes (the hybrid difference scheme and second-order HODIE) for the spatial derivative and the Euler-backward difference for the temporal derivative to discretize the problem (1).

3.1 The uniform mesh

In the time domain interval $[0, \mathscr{T}]$, we employ a uniform mesh with a time step $\Delta\theta$, ensuring that

$$\Lambda_\theta^{\mathscr{M}} = \{\theta_k = k\Delta\theta, \quad k = 0, \ 1, \ \ldots, \ \mathscr{M}, \quad \Delta\theta = \frac{\mathscr{T}}{\mathscr{M}}\},$$

Here, $\mathscr{M}$ represents the number of mesh points in the θ-direction within the interval $[0, \mathscr{T}]$.

3.2 Spatial discretization

We generate a modified graded mesh, $\Lambda_r^{\mathscr{N}}$ in the interval $[0, 1]$ and order to resolve the boundary layer at $r = 1$, which is plotted in Figure 1 as follows:

$$\sigma_i = 1 - \chi_{\mathscr{N}-1} \quad for \quad i = 1, \ldots, \mathscr{N},$$

where χ is defined as follows:

$$\begin{cases} \chi_0 = 0, \\ \chi_i = 2\varepsilon\frac{i}{\mathscr{N}}, & 1 \leq i \leq \frac{\mathscr{N}}{2}, \\ \chi_{i+1} = \chi_i(1 + \rho h), & \frac{\mathscr{N}}{2} \leq i \leq \mathscr{N} - 2, \\ \chi_{\mathscr{N}} = 1, \end{cases} \quad (10)$$

where the parameter h satisfies the following nonlinear equation:

$$\ln(1/\varepsilon) = (\mathscr{N}/2)\ln(1 + \rho h). \tag{11}$$

The above section of the parameter h ensures that there are $\mathscr{N}/2$ grid points in the interval $[0, 1-\varepsilon]$, which are distributed gradedly in the interval $[0, 1-\varepsilon]$. Numerical verification stimulate us that the interval $(\chi_{\mathscr{N}-1}, 1)$ is not too small in comparison with the previous one $(\chi_{\mathscr{N}-2}, \chi_{\mathscr{N}-1})$. In the subinterval $[1-\varepsilon, 1]$ we distribute $\mathscr{N}/2$ points with uniform step length $2\varepsilon/\mathscr{N}$, while in the subinterval $[0, 1-\varepsilon]$ we first find h for some fix $\mathscr{N}$ by means of the nonlinear equation (11), and corresponding to that h we distribute $\mathscr{N}/2$ points in the interval $[0, 1-\varepsilon]$. The mesh length is denoted by $h_i = \chi_i - \chi_{i-1}$, for $i = 1, 2, \ldots, \mathscr{N}$.

Remark 3. The mesh size in piecewise uniform and the modified graded region is given by

$$h_i = \begin{cases} 2\varepsilon/\mathscr{N} & \text{for } i = 1, 2, \ldots, \mathscr{N}/2, \\ \rho h \chi_{i-1} & \text{for } i = \mathscr{N}/2+1, \mathscr{N}/2+2, \ldots, \mathscr{N}. \end{cases}$$

Lemma 1. The mesh defined in (10) satisfies the following estimates:

$$|h_{i+1} - h_i| \leq \begin{cases} 0 & \text{for } i = 1, 2, \ldots, \mathscr{N}/2, \\ \mathscr{C}h & \text{for } i = \mathscr{N}/2+1, \mathscr{N}/2+2, \ldots, \mathscr{N}. \end{cases}$$

Proof. Initially, we consider $i = 1, 2, \ldots, \mathscr{N}/2$. As the mesh is uniform in this portion, so nothing to prove.

For $i = \mathscr{N}/2+1, \mathscr{N}/2+2, \ldots, \mathscr{N}$. We have

$$\begin{aligned} |h_{i+1} - h_i| &= |\rho h \chi_i - \rho h \chi_{i-1}| \\ &= \rho h |\chi_i - \chi_{i-1}| \\ &= \rho^2 h^2 \chi_{i-1} \\ &\leq \mathscr{C}h. \end{aligned}$$

Here, we have taken $0 < \rho, h < 1$. $\qquad\qquad\qquad\qquad\qquad\qquad\qquad\square$

Lemma 2. For the modified graded mesh defined in (10), the parameter h satisfies the following bound:

$$h \leq \mathscr{C} \mathscr{N}^{-1} \ln(1/\varepsilon).$$

Proof. Let $\mathscr{K}_1$ be the number of points χ_i in the partition (10) such that $\chi_i \leq \varepsilon$, for $i = 1, 2, \ldots, \mathscr{N}/2$. Clearly $\mathscr{K}_1 \leq \mathscr{C}/h$ and $\mathscr{K}_2$ be the number of points in the partition (10) such that $\chi_i > \varepsilon$. Let $\chi_{\mathscr{N}/2+1}$ be the smallest point such that $\chi_i > \varepsilon$. We have to estimate the bound for $\mathscr{K}_2$. Assuming $\rho h \leq 1$, we have

$$
\begin{aligned}
\mathscr{K}_2 &= \sum_{\mathscr{N}/2+1}^{\mathscr{N}} 1 = \sum_{\mathscr{N}/2+1}^{\mathscr{N}} (\chi_{i+1} - \chi_i)^{-1} \int_{\chi_i}^{\chi_{i+1}} d\chi \\
&= \sum_{\mathscr{N}/2+1}^{\mathscr{N}} (h_{i+1})^{-1} \int_{\chi_i}^{\chi_{i+1}} d\chi \\
&= \sum_{\mathscr{N}/2+1}^{\mathscr{N}} (\rho h \chi_i)^{-1} \int_{\chi_i}^{\chi_{i+1}} d\chi \\
&\leq \sum_{\mathscr{N}/2+1}^{\mathscr{N}} (2/\rho h \chi_{i+1})^{-1} \int_{\chi_i}^{\chi_{i+1}} d\chi,
\end{aligned}
$$

because $\chi_{i+1} < 2\chi_i$. For any $\chi \in [\chi_i, \chi_{+1}]$, we have

$$
\begin{aligned}
\mathscr{K}_2 &\leq \sum_{\mathscr{N}/2+1}^{\mathscr{N}} 2(\rho h)^{-1} \int_{\chi_i}^{\chi_{i+1}} \frac{1}{\chi} d\chi \\
&\leq 2(\rho h)^{-1} \int_{\varepsilon}^{1} \frac{1}{\chi} d\chi \\
&\leq 2(\rho h)^{-1} \ln(1/\varepsilon).
\end{aligned}
$$

Recalling $\mathscr{N} = \mathscr{K}_1 + \mathscr{K}_2$, we have

$$
\begin{aligned}
\mathscr{N} &\leq \mathscr{C}/\rho h + 2(\rho h)^{-1} \ln(1/\varepsilon), \\
\mathscr{N} &\leq 1/h(\mathscr{C}\rho + 2(\rho)^{-1} \ln(1/\varepsilon)), \\
\mathscr{N} &\leq 1/h(\mathscr{C} \ln(1/\varepsilon)),
\end{aligned}
$$

Finally, we get

$$h \leq \mathscr{C} \mathscr{N}^{-1} \ln(1/\varepsilon),$$

where $\mathscr{N}$ is the number of grid points in the r-direction.   □

(a) $N = 32, \varepsilon = 10^{-1}$ (b) $N = 128, \varepsilon = 10^{-2}$
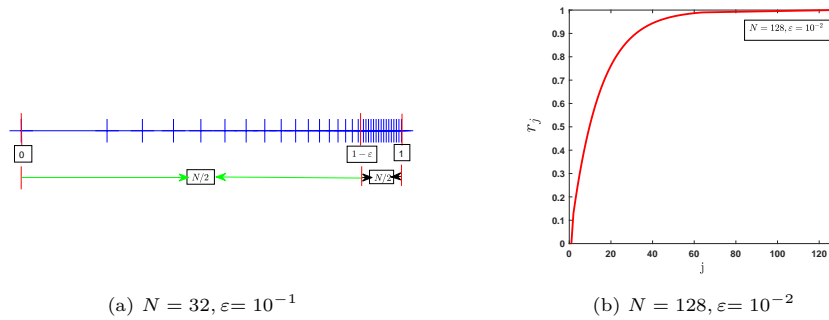
Figure 1: Distribution of modified graded mesh points for the problems with the layer on the right side of the boundary, that is, $r = 1$, which is plot in Figure 1.

Figure 1a shows the distribution of the domain $[0, 1]$, while Figure 1b illustrates the layer within the domain $[0, 1]$.

3.3 The finite difference scheme

In this section, we used the backward-Euler difference in the time direction and two finite difference schemes (the hybrid midpoint method and the HODIE method) for the spatial direction on the modified graded mesh. Now, a free parameter p_i^1 that is defined by the following, is utilized to characterize the second-order HODIE finite difference scheme of [3], which is used to discretize the spatial derivative of (1):

$$p_i^1 = \begin{cases} \frac{d_i}{d_{i-1} + d_i} & \text{for } i = 1, 2, 3, \ldots, \mathscr{N}/2, \\ 0, & \text{for } i = \mathscr{N}/2 + 1, \ldots, \mathscr{N} - 1. \end{cases} \tag{12}$$

Here, we suppose that $\mathscr{H}||d||_\infty \geq 2\varepsilon$ (see [3]). Let us denote the step sizes in space by $h_i := r_i - r_{i-1}$ and $\hat{h}_i := (h_i + h_{i+1})/2$ for all i, and $\Delta\theta = \theta_j - \theta_{j-1}$

for all j. Then, Y_i^j is the analytical solution at the grid point (r_i, θ_i), and also we define the HODIE and midpoint difference scheme of [3] is

$$p_i^1 \frac{Y_{i-1}^j - Y_{i-1}^{j-1}}{\Delta\theta} + (1 - p_i^1)\frac{Y_i^j - Y_i^{j-1}}{\Delta\theta} + [\mathscr{L}_\varepsilon^{\mathscr{N},\mathscr{M}}Y]_i^j = p_j^1 f_{i-1}^j + (1 - p_i^1)f_i^j \tag{13a}$$

for $i = 1, 2, 3, \ldots, \mathscr{N}/2$, and

$$\frac{Y_i^j - Y_i^{j-1}}{\Delta\theta} + [\mathscr{L}_\varepsilon^{\mathscr{N},\mathscr{M}}Y]_i^j = f_i^j, \quad \text{for} \quad i = \mathscr{N}/2 + 1, \ldots, \mathscr{N} - 1, \tag{13b}$$

where

$$\mathscr{L}_\varepsilon^{\mathscr{N},\mathscr{M}}Y]_i^j = q_{ij}^- Y_{i-1}^j + q_{ij}^c Y_i^j + q_{ij}^+ Y_{i+1}^j \tag{13c}$$

with

$$\begin{cases} q_{ij}^- = -\dfrac{\varepsilon}{h_i \hat{h}_i} - \dfrac{2p_i^1 d_{i-1}}{h_i} + p_i^1 \kappa_{2i-1}^j, \\[2mm] q_{ij}^+ = -\dfrac{\varepsilon}{h_{i+1}\hat{h}_i}, \\[2mm] q_{ij}^c = -q_{ij}^- - q_{ij}^+ + p_i^1 \kappa_{2i-1}^j + (1 - p_i^1)\kappa_{2i}^j \end{cases} \tag{13d}$$

for $i = 1, 2, 3, \ldots, \mathscr{N}/2$, and

$$\begin{cases} q_{ij}^- = -\dfrac{\varepsilon}{h_i \hat{h}_i} - \dfrac{d_i}{2\hat{h}_i}, \\[2mm] q_{ij}^+ = -\dfrac{\varepsilon}{h_{i+1}\hat{h}_i} + \dfrac{d_i}{2\hat{h}_i}, \\[2mm] q_{ij}^c = -q_{ij}^- - q_{ij}^+ + \kappa_{2i}^j \end{cases} \tag{13e}$$

for $i = \mathscr{N}/2 + 1, \ldots, \mathscr{N} - 1$.

When $i = 1, 2, 3, \ldots, \mathscr{N}/2$, it is easy to see that

$$p_i^1 = \frac{1}{2} + O(h_i), \quad \text{and} \quad 2p_i^1 d_{i-1} = d_{i-1/2} + O(h_i^2), \tag{14}$$

where $d_{i-1/2} := (d_{i-1} + d_i)/2$. thus, replacing $2p_i^1 d_{i-1}$ by $d_{i-1/2}$ in (13d) and p_i^1 by $1/2$ elsewhere, the scheme (13) becomes

$$\frac{1}{2}\left(\frac{Y_{i-1}^j - Y_{i-1}^{j-1}}{\Delta\theta}\right) + \frac{1}{2}\left(\frac{Y_i^j - Y_i^{j-1}}{\Delta\theta}\right) + [\mathscr{L}_\varepsilon^{\mathscr{N},\mathscr{M}}Y]_i^j = \frac{1}{2}(f_{i-1}^j + f_i^j), \tag{15a}$$

for $i = 1, 2, 3, \ldots, \mathscr{N}/2$, and

$$\frac{Y_i^j - Y_i^{j-1}}{\Delta\theta} + [\mathscr{L}_\varepsilon^{\mathscr{N},\mathscr{M}}Y]_i^j = f_i^j, \quad \text{for} \quad i = \mathscr{N}/2 + 1, \ldots, \mathscr{N} - 1, \quad (15b)$$

where

$$[\mathscr{L}_\varepsilon^{\mathscr{N},\mathscr{M}}Y]_i^j = q_{ij}^- Y_{i-1}^j + q_{ij}^c Y_i^j + q_{ij}^+ Y_{i+1}^j, \quad (15c)$$

with

$$\begin{cases} q_{ij}^- = -\dfrac{\varepsilon}{h_i\hat{h}_i} - \dfrac{d_{i-1/2}}{h_i} + \dfrac{1}{2}\kappa_2{}_{i-1}^j, \\[2mm] q_{ij}^+ = -\dfrac{\varepsilon}{h_{i+1}\hat{h}_i}, \\[2mm] q_{ij}^c = -q_{ij}^- - q_{ij}^+ + \dfrac{1}{2}\kappa_2{}_{i-1}^j + \dfrac{1}{2}\kappa_2{}_i^j \end{cases} \quad (15d)$$

for $i = 1, 2, 3, \ldots, \mathscr{N}/2,$ and

$$\begin{cases} q_{ij}^- = -\dfrac{\varepsilon}{h_i\hat{h}_i} - \dfrac{d_i}{2\hat{h}_i}, \\[2mm] q_{ij}^+ = -\dfrac{\varepsilon}{h_{i+1}\hat{h}_i} + \dfrac{d_i}{2\hat{h}_i}, \\[2mm] q_{ij}^c = -q_{ij}^- - q_{ij}^+ + \kappa_2{}_i^j \end{cases} \quad (15e)$$

for $i = \mathscr{N}/2 + 1, \ldots, \mathscr{N} - 1,$

According to the description above, the numerical solution of the problems (1) in section 5 will demonstrate that the schemes (13) and (15) provide outcomes that are almost equal.

4 Analysis of the uniform convergence

In this section, we aim to establish uniform convergence using a new concept involving modified graded meshes. Our examination will focus on the hybrid midpoint finite difference method (15). This choice is made due to the relatively simpler coefficients in the midpoint finite difference scheme compared to the HODIE finite difference scheme (13). It is important to note that the analysis presented here for the hybrid midpoint finite difference method can be readily extended to apply to the HODIE finite difference scheme (13). The analysis of the schemes (15) and (13) will be second order of convergence with respect to the perturbation parameter , and also show that the schemes (15) and (13) are identical.

Lemma 3. Assume that

$$\eta||d||_\infty < \frac{\mathcal{N}}{\ln(1/\varepsilon)} \quad \text{and} \quad \lambda\mathcal{N} \geq (||\kappa_2||_\infty + (\Delta\theta)^{-1}). \tag{16}$$

Then, the coefficient of (15) satisfies the following for every j:

(a) $q_{ij}^+ \leq 0$, (b) $q_{ij}^- + (2\Delta\theta)^{-1} \leq 0$ and (c) $q_{ij}^c + (2\Delta\theta)^{-1} \geq 0$, for $i = 1, 2, 3, \ldots, \mathcal{N}/2$,

(d) $q_{ij}^- \leq 0$, (e) $q_{ij}^c + (\Delta\theta)^{-1} \geq 0$, and (f) $q_{ij}^+ \leq 0$ for $i = \mathcal{N}/2 + 1, \ldots, \mathcal{N} - 1$.

Moreover, the tridiagonal matrix associated with computing the discrete solution at each time level θ_j is an M-matrix.

Proof. In the case of $1 \leq i \leq \mathcal{N}/2$, the proofs are provided as follows. Since $q_{ij}^+ = -\dfrac{\varepsilon}{h_{i+1}\hat{h}_i}$, which is less than zero for all i, j. Therefore we have $q_{ij}^+ \leq 0$, hence the result (a). In order to prove the result (b), we observe that the term $q_{ij}^- + (2\Delta\theta)^{-1}$ satisfies

$$\begin{aligned}
q_{ij}^- + (2\Delta\theta)^{-1} &= -\frac{\varepsilon}{h_i\hat{h}_i} - \frac{d_{i-1/2}}{h_i} + \frac{1}{2}\kappa_{2i-1}^j + \frac{1}{2\Delta\theta} \\
&\leq -\frac{\varepsilon}{h_i\hat{h}_i} - \frac{d_{i-1/2}}{h_i} + \frac{1}{2}\kappa_{2i-1}^j + \frac{1}{2}(||\kappa_2|| + (\Delta\theta)^{-1}) \\
&\leq -\frac{\varepsilon}{h_i\hat{h}_i} - \frac{d_{i-1/2}}{h_i} + \frac{1}{2}\kappa_{2i-1}^j + \lambda\mathcal{N}, \\
&\quad \text{using } \lambda\mathcal{N} \geq ||\kappa_2|| + (\Delta\theta)^{-1} \text{ and } (16).
\end{aligned}$$

The inequality $\kappa_1(r) > \lambda > 0$ implies that $\lambda < d_i$ as well as $\lambda < d_{i-1}$. Therefore we have, $2\lambda < \kappa_{1i} + \kappa_{1i-1}$, that is $\lambda < \dfrac{\kappa_{1i} + \kappa_{1i-1}}{2}$. Moreover, $\kappa_{1i-1/2}\dfrac{\lambda}{h_i} < \dfrac{\kappa_{1i-1/2}}{h_i}$ results $\lambda\mathcal{N} < \dfrac{\lambda}{h_i} < \dfrac{\kappa_{1i-1/2}}{h_i}$, which leads to the inequality $\lambda\mathcal{N} < \dfrac{\kappa_{1i-1/2}^-}{h_i} < 0$, thus we have $q_{ij}^- + (2\Delta\theta)^{-1} \leq 0$, which proves the result in the case of $1 \leq i \leq \mathcal{N}/2$.

From (15d), we get

$$\begin{aligned}
q_{ij}^c + (2\Delta\theta)^{-1} &= -q_{ij}^- - q_{ij}^+ + \frac{1}{2}\kappa_{2i-1}^j + \frac{1}{2}\kappa_{2i}^j \\
&= \frac{\varepsilon}{h_i\hat{h}_i} + \frac{a_{i-1/2}}{h_i} - \frac{1}{2}\kappa_{2i-1}^j + \frac{\varepsilon}{\hat{h}_ih_{i+1}} + \frac{1}{2}\kappa_{2i-1}^j + \frac{1}{2}\kappa_{2i}^j
\end{aligned}$$

$$= \frac{\varepsilon}{\hat{h}_i}\left(\frac{h_{i+1}+h_i}{h_{i+1}h_i}\right) + \frac{\kappa_{1i-1/2}}{h_i} + \frac{1}{2}\kappa_{2i}^j \geqslant 0.$$

Hence, $q_{ij}^- + (2\Delta\theta)^{-1} \geq 0$. Thus we have the result (c).

In the case of $i = \mathcal{N}/2+1, \ldots, \mathcal{N}-1$, the results are provided as follows. From (15e), it follows that $q_{ij}^- \leq 0$ since $q_{ij}^- = -\frac{\varepsilon}{h_i\hat{h}_i} - \frac{d_i}{2\hat{h}_i}$, Hence we have established the result (d), that is, $q_{ij}^- \leq 0$.

Observing from $(15e)$, we have

$$-q_{ij}^- - q_{ij}^+ + \kappa_{2i}^j + (\Delta\theta)^{-1} = \frac{\varepsilon}{h_i\hat{h}_i} + \frac{d}{2\hat{h}_i} + \frac{\varepsilon}{h_{i+1}\hat{h}_i} - \frac{d}{2\hat{h}_i} + \kappa_{2i}^j + \frac{1}{\Delta\theta} \geq 0.$$

Therefore, $q_{ij}^c + (\Delta\theta)^{-1} \geq 0$. Hence we have established the result (e).

In order to prove the result (f), we note that

$$\begin{aligned}
q_{ij}^+ &= -\frac{\varepsilon}{h_{i+1}\hat{h}_i} + \frac{d_i}{2\hat{h}_i} \leq \frac{\varepsilon}{h_{i+1}\hat{h}_i} + \frac{||d_i||}{2\hat{h}_i} \\
&\leq \frac{\varepsilon}{h_{i+1}\hat{h}_i} + \frac{\mathcal{N}}{\ln(1/\varepsilon)}\frac{1}{2\hat{h}_i} = \frac{\varepsilon}{h_{i+1}\hat{h}_i} + \frac{\mathcal{N}\varepsilon}{(1-\varepsilon)}\frac{1}{2\hat{h}_i} \\
&= \frac{-\varepsilon}{\hat{h}_i}\left(\frac{1}{h_{i+1}} - \frac{\mathcal{N}}{2(1-\varepsilon)}\right).
\end{aligned}$$

From the inequality $\dfrac{1}{\mathcal{N}} > h_{i+1}$ it is straight forward to observe that $\dfrac{\mathcal{N}}{2(1-\varepsilon)} < \dfrac{1}{h_{i+1}}$. Substituting this in the previous inequality we obtain $q_{ij}^+ \leq 0$, which proves the result for the case (f). This completes the proof. $\square$

Assuming the validity of (16), we proceed to establish that Lemma 3 implies the existence of a unique solution for the scheme (15) at each time level. Furthermore, the solution adheres to a discrete maximum principle. By incorporating the maximum principle with a barrier function expressed as $\mathscr{C}(1+r)$, a priori bound $||Y||_{\infty,d} \leq \mathscr{C}||f||_\infty$ with a constant $\mathscr{C}$ is derived. Here, the discrete maximum norm is defined as $||z||_{\infty,d} := \max\limits_{i,j}|z_i^j|$ for each mesh function z.

Now, we will presented our main result. To obtain the estimation we will follow the Koptewa's methodology [13, 14] and also the result presented in [16].

Theorem 1. Assume (16) is valid. Then there exists a constant $\mathscr{C}$ such that

$$\max_{i,j} |y(r_i, \theta_j) - Y_i^j| \leq \mathscr{C}[\Delta\theta + \varepsilon \mathscr{N}^{-1} + (\mathscr{N}^{-1} \ln(1/\varepsilon))^2]. \tag{17}$$

Proof. Suppose that $\zeta_i^j = y_i^j - Y_i^j$ is the error of discrete solution of the problem (1) on the modified graded mesh applied the scheme (15) at each grid point (r_i, θ_j). We can write the scheme of midpoint, which is given in (15) as

$$[\tilde{\gamma}_\theta Y]_i^j + [\mathscr{L}_\varepsilon^{\mathscr{N},\mathscr{M}} Y]_i^j = \hat{f}_i^j \ \text{ for } i = 1, 2, 3, \ldots, \mathscr{N}-1, \text{ and } j = 1, \ldots, \mathscr{M}, \tag{18}$$

where

$$\hat{f}_i^j = \begin{cases} \dfrac{1}{2}[f(r_{i-1}, \theta_j) + f(r_i, t_j)] & \text{if } i \leq \frac{\mathscr{N}}{2}, \ j \leq \frac{\mathscr{M}}{2}, \\ f(r_i, \theta_j) & \text{if } i > \frac{\mathscr{N}}{2}, \ j > \frac{\mathscr{M}}{2}, \end{cases} \tag{19}$$

and the backward difference operator $\tilde{\gamma}_\theta$ can be defined analogously. Therefore, at each point $(r_i, \theta_j) \in \Lambda$, the truncation error of the scheme is

$$[\tilde{\gamma}_\theta \zeta + \mathscr{L}_\varepsilon^{\mathscr{N},\mathscr{M}} \zeta]_i^j = \vartheta_{1;i}^j + \vartheta_{2;i}^j, \tag{20}$$

where

$$\vartheta_{1;i}^j := [\mathscr{L}_\varepsilon^{\mathscr{N},\mathscr{M}} y]_i^j - (\overline{\mathscr{L}}_\varepsilon y)_i^j \ \text{ and } \ \vartheta_{2;i}^j := \tilde{\gamma}_\theta y_i^j - (\tilde{y}_\theta)_i^j \tag{21}$$

with $(\tilde{y}_\theta)_i^j$ define similarly to (19), and

$$(\overline{\mathscr{L}}_\varepsilon y)_i^j = \begin{cases} \dfrac{1}{2}[(\mathscr{L}_\varepsilon y)(r_{i-1}, \theta_j) + (\mathscr{L}_\varepsilon y)(r_i, \theta_j)], & \text{if } i \leq \mathscr{N}/2, \\ (\mathscr{L}_\varepsilon y)(r_i, \theta_i), & \text{if } i > \mathscr{N}/2. \end{cases}$$

Decompose ζ as $\zeta = \mu + \nu$. the functions $\{\mu_i^j\}$, $j = 0, \ldots, \mathscr{M}$ are the solutions to the discrete boundary value problem with two-point,

$$[\mathscr{L}_\varepsilon^{\mathscr{N},\mathscr{M}} \mu]_i^j = \vartheta_{1,i}^j \ \text{ for } \ i = 1, \ldots, \mathscr{N}-1, \ \ \mu_0^j = \mu_{\mathscr{N}}^j = 0, \tag{22}$$

while $\{\nu_i^j\}$ are the solution of a discrete parabolic problem defined by

$$[\tilde{\gamma}_\theta \nu + \mathscr{L}_\varepsilon^{\mathscr{N},\mathscr{M}} \nu]_i^j = \vartheta_{2;i}^j - \tilde{\gamma}_\theta \mu_i^j \ \text{ for } \ i = 1, \ldots, \mathscr{N} - 1, \qquad (23a)$$

with the boundary conditions

$$\nu_0^j = \nu_{\mathscr{N}}^j = 0 \text{ for } j = 1, \ldots, \mathscr{M}, \qquad (23b)$$

and the initial condition

$$\nu_i^0 = -\nu_i^0 \text{ for } i = 0, \ldots, \mathscr{N}. \qquad (23c)$$

Equation (22) precisely represents the identity obtained when examining the error μ in a two-point boundary value problem that has undergone discretization using $\mathscr{L}_\varepsilon$, with $\vartheta_{1;i}^j$ serving as the truncation error. Utilized the bound (6) with the value of $l = 0$, we obtained the same bound on the $\vartheta_{1;i}^j$ as for a convection-diffusion two point boundary value problems. As a result, it is possible to use the error bound determined in [20],

$$|\mu_i^j| \le \mathscr{C}[\varepsilon \mathscr{N}^{-1} + (\mathscr{N}^{-1} \ln(1/\varepsilon))^2] \text{ for all } i, j. \qquad (24)$$

Again, we include the one-more error component ν. Lemma 1 implies that the problem (23) satisfies a discrete maximum principle just as (15) does, so

$$||\nu||_{\infty,d} \le \mathscr{C}\left(\max_i |\mu_i^0| + \|\vartheta_2 - \tilde{\gamma}_\theta \mu\|_{\infty,d} \right)$$

$$\le \mathscr{C}[\Delta\theta + \varepsilon \mathscr{N}^{-1} + (\mathscr{N}^{-1} \ln(1/\varepsilon))^2 + \|\tilde{\gamma}_\theta \mu\|_{\infty,d}], \qquad (25)$$

where we used (24) with $j = 0$ and also

$$|\vartheta_{2;i}^j| \le \mathscr{C}\Delta\theta \ \text{ for } \ i = 1, \ldots, \mathscr{N} - 1, \ \text{ and } \ j = 1, \ldots, \mathscr{M}, \qquad (26)$$

The verification has been completed using Taylor's series expansion and (6). It remains to estimate $\tilde{\gamma}_\theta \mu$ appears in (23). Utilizing the assumption that $\kappa_1 = \kappa_1(r)$ is independent of θ, a straightforward calculation reveals that, for each fixed j, the definition (22) implies satisfaction for $\tilde{\gamma}_\theta \mu$

$$[\mathscr{L}_\varepsilon^{\mathscr{N},\mathscr{M}} (\tilde{\gamma}_\theta \mu)]_i^j = \tilde{\gamma}_\theta \vartheta_{1;i}^j - ((\tilde{\gamma}_\theta \kappa_2)\mu^{j-1})_i \ \text{ for } \ i = 1, \ldots, \mathscr{N} - 1, \qquad (27a)$$

$$(\tilde{\gamma}_\theta \mu)_0^j = (\tilde{\gamma}_\theta \mu)_{\mathcal{N}}^j = 0, \tag{27b}$$

The notation $()_i$ employed here carries the same meaning as in (18).

Based on the decomposition $\gamma_\theta \mu = \Phi + \Psi$, wherein, for each fixed $j \in 1, 2, \ldots, \mathcal{M}$, the following relationship holds:

$$[\mathscr{L}_\varepsilon^{\mathcal{N},\mathcal{M}} \Phi]_i^j = \tilde{\gamma}_\theta \vartheta_{1;i}^j \ \text{ for } \ i = 1, \ldots, \mathcal{N} - 1 \ \text{ with } \ \Phi_0^j = \Phi_{\mathcal{N}}^j = 0, \tag{28a}$$

$$[\mathscr{L}_\varepsilon^{\mathcal{N},\mathcal{M}} \Psi]_i^j = -((\tilde{\gamma}_\theta \kappa_2)\mu^{j-1})_i \ \text{ for } \ i = 1, \ldots, \mathcal{N} - 1 \ \text{ with } \ \Psi_0^j = \Psi_{\mathcal{N}}^j = 0. \tag{28b}$$

To examine the discrete two-point boundary value problem (28a), an analysis will be conducted and observe that for $i \leq \mathcal{N}/2$ the right-hand side of (28a) is

$$\begin{aligned}
\tilde{\gamma}_\theta \vartheta_{1;i}^j =& \frac{1}{2\Delta\theta}(\vartheta_{1;i-1}^j - \vartheta_{1;i-1}^{j-1}) + \frac{1}{2\Delta\theta}(\vartheta_{1;i}^j - \vartheta_{1;i}^{j-1}) \\
=& \frac{1}{2\Delta\theta}[([\mathscr{L}_\varepsilon^{\mathcal{N},\mathcal{M}} y]_{i-1}^j - [\mathscr{L}_\varepsilon^{\mathcal{N},\mathcal{M}} y]_{i-1}^{j-1}) - ([\mathscr{L}_\varepsilon y]_{i-1}^j - [\mathscr{L}_\varepsilon y]_{i-1}^{j-1})] \\
&+ \frac{1}{2\Delta\theta}[([\mathscr{L}_\varepsilon^{\mathcal{N},\mathcal{M}} y]_i^j - [\mathscr{L}_\varepsilon^{\mathcal{N},\mathcal{M}} y]_i^{j-1}) - ([\mathscr{L}_\varepsilon y]_i^j - [\mathscr{L}_\varepsilon y]_i^{j-1})].
\end{aligned}$$

Set $\overline{\mathscr{L}}_\varepsilon y = -\varepsilon y_{rr} + \kappa_1 y_r$. Let $[\overline{\mathscr{L}}_\varepsilon^{\mathcal{N},\mathcal{M}} Y]_i^j$ be defined by setting $\kappa_2 \equiv 0$ in $[\mathscr{L}_\varepsilon^{\mathcal{N},\mathcal{M}} y]_i^j$ for all i, j; that is, $\overline{\mathscr{L}}_\varepsilon^{\mathcal{N},\mathcal{M}}$ is the discretization of $\overline{\mathscr{L}}_\varepsilon$. Then for $i \leq \mathcal{N}/2$, we can expressed the above formula in the form

$$\begin{aligned}
\tilde{\gamma}_\theta \vartheta_{1;i}^j =& \frac{1}{2\Delta\theta} \int_{\theta_{j-1}}^{\theta_j} [(\overline{\mathscr{L}}_\varepsilon^{\mathcal{N},\mathcal{M}} y_\theta(r_{i-1}, \theta) + \overline{\mathscr{L}}_\varepsilon^{\mathcal{N},\mathcal{M}} y_\theta(r_i, \theta)) \\
&- (\overline{\mathscr{L}}_\varepsilon y_\theta(r_{i-1}, \theta) + \overline{\mathscr{L}}_\varepsilon y_\theta(r_i, \theta))]d\theta.
\end{aligned}$$

It is important to note that here we employed the assumption that $\kappa_1 = \kappa_2(r)$ is not dependent on θ, since this yields $\overline{\mathscr{L}}_\varepsilon y_\theta = (\overline{\mathscr{L}}_\varepsilon y)_\theta$. Hence, we employed the Peano kernel theorem that is also used in the article [12], and we get

$$\begin{aligned}
|\tilde{\gamma}_\theta \vartheta_{1;i}^j| =& \mathscr{C}\varepsilon \int_{r_{i-1}}^{r_{i+1}} \max_{\theta \in [\theta_{j-1}, \theta_j]} |y_{rrr\theta}(r, \theta)|d\theta \\
&+ \mathscr{C} h_i \int_{r_{i-1}}^{r_i} \max_{\theta \in [\theta_{j-1}, \theta_j]} (|y_{r\theta}| + |y_{rr\theta}| + |y_{rrr\theta}|)(r, \theta)d\theta.
\end{aligned}$$

The bounds of (8) are unaffected by the addition of the θ–derivative, resulting in an estimate that is equivalent to the corresponding truncation error limits appearing in [20] for a typical two-point boundary value problem. When $i \geq \mathscr{N}/2$, then the bound from the last inequality in the proof of a bound that is identical to the equivalent truncation error bound derivative [20]. These results show that analysis of (28a) may be performed in a similar manner to that of (22), with the exception that one utilizes the bound (8) with $l = 1$. We therefore obtain

$$|\Phi_i^j| \leq \mathscr{C}[\varepsilon \mathscr{N}^{-1} + (\mathscr{N}^{-1} \ln(1/\varepsilon))^2] \ \text{ for all } i \text{ and } j. \tag{29}$$

To handle (27b), note that $\mathscr{L}_\varepsilon$ is an M-matrix and therefore fulfills the discrete maximum principle. The easy conclusion that one has to satisfy for every j

$$\begin{aligned}
\max_i |\Psi_i^j| &\leq C \max_i |((\tilde{\gamma}_\theta b)\mu^{j-1})_i| \\
&\leq \mathscr{C} \max_i |\mu_i^{j-1}| \leq \mathscr{C}[\varepsilon \mathscr{N}^{-1} + (\mathscr{N}^{-1} \ln(1/\varepsilon))^2],
\end{aligned} \tag{30}$$

where we used $|\tilde{\gamma}_\theta \kappa_2| \leq \mathscr{C}$ and (24).

Combining (24), (25), (29), and (30), we get (17)

$$\max_{i,j} |y(r_i, \theta_j) - Y_i^j| \leq \mathscr{C}[\Delta\theta + \varepsilon \mathscr{N}^{-1} + (\mathscr{N}^{-1} \ln(1/\varepsilon))^2].$$

and Theorem 1 also holds true for the scheme (13). This completes the proof. $\qquad\qquad\square$

5 Examples and their numerical results

In this section, we shall present the numerical results obtained by the two finite difference schemes, the hybrid midpoint method (15) and the HODIE method (13) of the problem (1) on the modified graded mesh and also calculate the maximum point-wise error and order of convergence with the different values of ε and $\mathscr{N}, \mathscr{M}$. We tackled two Examples to showcase the effectiveness and efficiency of the proposed schemes. It's important to note that this

article does not provide an exact solution for Examples 1 and 2. Instead, we employ the double mesh approach outlined below to assess the maximum point-wise errors and determine the order of convergence. We demonstrate the efficiency of the proposed numerical scheme by two examples to show that the schemes (13) and (15) yield very similar results and confirm the convergence estimate of Theorem 1.

Example 1. Consider the following parabolic initial-boundary value problem:

$$
\begin{cases}
y_\theta - \varepsilon y_{rr} + \left(1 + r^2 + \dfrac{\sin(\pi r)}{2}\right) y_r + (1 + r^2 + \sin(\pi\theta))y = f(r,\theta), \\
f(r,\theta) = r^3(1-r)^3 + \theta(1-\theta)\sin(\pi\theta), \quad \text{for} \quad (r,\theta) \in (0,1) \times (0,1), \\
y(0,\theta) = y(1,\theta) = y(r,0) = 0 \quad \text{for} \quad (r,\theta) \in [0,1],
\end{cases} \tag{31}
$$

The exact solution of the $y(r,\theta)$ of (31) is not provided and also the results of this problem satisfy only the first-order and second-order corner compatibility conditions (4) and (5). The point-wise errors $|y(r_i,\theta_i) - Y_i^j|$ are obtained on the our mesh $\Lambda_{\mathcal{M},\mathcal{N}}$. The double mesh technique can also be found in the reference [3, 17]. That is a new approximate solution $\{\hat{Y}_i^j\}$ is computed using the same scheme but on the mesh the comprises the points of the original mesh and their midpoints $((r_{i-1}+r_i)/2, \theta_i), ((r_i, (\theta_{i-1}+\theta_i)/2)$ and $((r_{i-1}+r_i)/2, (\theta_{i-1}+\theta_i)/2)$. Thus, the values Y_i^j and $\hat{Y}_{2i}^{2j}$ are computed at the same physical point (r_i,θ_i) of $\Lambda_{\mathcal{M},\mathcal{N}}$. Then at the mesh points of the original mesh $\Lambda_{\mathcal{M},\mathcal{N}}$ one calculates the maximum and uniform two mesh differences defined by

$$
d_\varepsilon^{\mathcal{N},\mathcal{M}} = \max_{0 \le j \le \mathcal{M}} \max_{0 \le i \le \mathcal{N}} |Y_i^j - \hat{Y}_{2i}^{2j}|, \quad d^{\mathcal{N},\mathcal{M}} = \max_{\varepsilon \in S} d_\varepsilon^{\mathcal{N},\mathcal{M}}, \tag{32}
$$

where $S := \{2^{-3}, 2^{-6}, 2^{-9}, 2^{-12}, 2^{-15}, \ldots, 2^{-30}\}$. From these values one computes the order of convergence and the uniform orders of convergence in the standard way:

$$
p_\varepsilon^{\mathcal{N},\mathcal{M}} := \frac{\log(d_\varepsilon^{\mathcal{N},\mathcal{M}} / \log(d_\varepsilon^{2\mathcal{N},2\mathcal{M}})}{\log 2}, \quad p_{uni}^{\mathcal{N},\mathcal{M}} := \frac{\log(d^{\mathcal{N},\mathcal{M}} / \log(d^{2\mathcal{N},2\mathcal{M}})}{\log 2}.
$$

We employ the proposed schemes (15) and (13), the hybrid midpoint finite difference scheme and the HODIE finite difference scheme on the modified

---

graded mesh to solve the Examples 1 and 2 for different values of perturbation parameter ε with the spatial mesh grid size $\mathcal{N}$ and time grid size $\mathcal{M}$. We have also calculated the maximum point-wise errors and their corresponding order of convergent. From Tables 1 to 4, we can analyze that the proposed schemes (15) and (13) with the modified graded mesh are ε−uniformly convergent for distinct values of ε and $\mathcal{N}, \mathcal{M}$. Because of this as a result of this observation, we can assert that the computationally achieved order of convergence surpasses the one predicted in the preceding section. It has been demonstrated that the theoretical rate of convergence for the developed method is second order in the spatial direction and first order in the time direction. Besides, the comparison of numerical results obtained by the proposed scheme and results in [3] and [17] are tabulated in Tables 5 and 6 for Example 1. From these tables, one can conclude that the proposed scheme gives better results than the scheme considered in [3] and [17].

Figure 2 shows the numerical solution profile for Example 1 for various values of ε and step sizes $\mathcal{N}$ and $\mathcal{M}$ for schemes (13) and (15), respectively. The calculated maximum point-wise errors $d^{\mathcal{N},\mathcal{M}}$ and the corresponding order of convergence $p_{uni}^{\mathcal{N},\mathcal{M}}$ for Example 1 with schemes (13) and (15) on modified graded mesh are shown in Tables 1 and 2, respectively. From these results one can observe the ε-uniform second-order convergence of the numerical solution.

Example 2. Consider the following parabolic initial-boundary value problem:

$$
\begin{cases}
y_\theta - \varepsilon y_{rr} + \left(1 + r^2 + \dfrac{\sin(\pi r)}{2}\right)y_r + (1 + r^2 + \dfrac{1}{2}\sin(\pi\theta/2))y = f(r,\theta) \\
f(r,\theta) = r^3(1-r)^3\theta(1-\theta)\sin(\pi\theta), \quad \text{for} \quad (r,\theta) \in (0,1) \times (0,1) \\
y(0,\theta) = y(1,\theta) = y(r,0) = 0, \quad \text{for} \quad (r,\theta) \in [0,1],
\end{cases}
\tag{33}
$$

for which the exact solution is again unknown. Similarly, numerical solution profiles for Example 2 for various values of ε and step sizes $\mathcal{N}$ and $\mathcal{M}$ are provided in Figure 3 for the schemes (13) and (15). The results reveal the presence of a boundary layer on the right side of the domain. The calculated maximum point-wise errors $d^{\mathcal{N},\mathcal{M}}$ and the corresponding order of convergence $p_{uni}^{\mathcal{N},\mathcal{M}}$ for Example 2 with schemes (13) and (15) on modified

graded mesh are shown in Tables 3 and 4, respectively. From these results one can observe the ε-uniform second-order convergence of the numerical solution. The maximum point-wise errors are plotted in log-log scale in Figure 4, for the solution. From these figures,one can easily observe the second-order ε-uniform convergence.
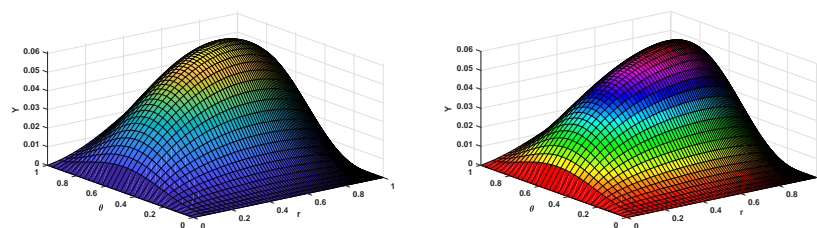
(a) $\mathcal{N} = 128, \mathcal{M} = 32, \varepsilon = 10^{-3}$, Scheme (13)(b) $\mathcal{N} = 128, \mathcal{M} = 32, \varepsilon = 10^{-3}$, Scheme (15)

Figure 2: Solution profile for Example 1 using schemes (13) and (15) on modified graded mesh
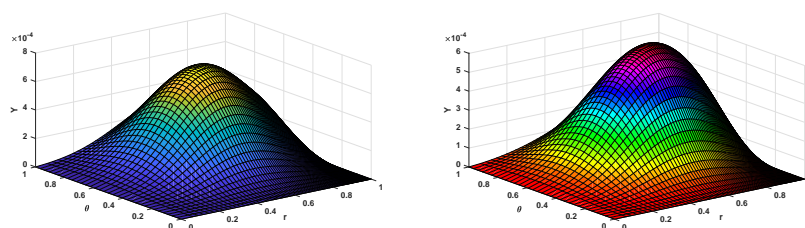
(a) $\mathcal{N} = 128, \mathcal{M} = 32, \varepsilon = 10^{-3}$, Scheme (13)(b) $\mathcal{N} = 128, \mathcal{M} = 32, \varepsilon = 10^{-3}$, Scheme (15)

Figure 3: Solution profile for Example 2 using schemes (13) and (15) on modified graded mesh.

Table 1: *Maximum point-wise errors and the corresponding order of convergence for Example 1 on a modified graded mesh using scheme* (13)

	Number of Intervals $\mathcal{N}, \mathcal{M}$				
	$\mathcal{N} = 84$	$\mathcal{N} = 168$	$\mathcal{N} = 336$	$\mathcal{N} = 672$	$\mathcal{N} = 1344$
ε	$\mathcal{M} = 5$	$\mathcal{M} = 20$	$\mathcal{M} = 80$	$\mathcal{M} = 320$	$\mathcal{M} = 1280$
2^{-3}	$9.4000e-03$	$2.7000e-03$	$6.9703e-04$	$1.7986e-04$	$4.7299e-05$
	1.8260	1.9338	1.9544	1.9270	
2^{-6}	$1.1000e-03$	$3.6000e-03$	$1.0000e-03$	$2.8406e-04$	$8.2442e-05$
	1.6292	1.8075	1.8428	1.7847	
2^{-9}	$1.1100e-03$	$3.8000e-03$	$1.2000e-03$	$3.6372e-04$	$1.1823e-04$
	1.5443	1.6842	1.7058	1.6212	
2^{-12}	$1.0700e-03$	$3.7000e-03$	$1.2000e-03$	$3.9593e-04$	$1.3800e-04$
	1.5221	1.6259	1.6130	1.5205	
2^{-15}	$1.0400e-03$	$3.6000e-03$	$1.3000e-03$	$4.7031e-04$	$1.5294e-04$
	1.5315	1.4188	1.5127	1.6206	
2^{-18}	$1.0500e-03$	$3.8000e-03$	$1.7000e-03$	$6.3183e-04$	$1.9519e-04$
	1.4580	1.1733	1.4249	1.6947	
2^{-21}	$1.2500e-03$	$4.7000e-03$	$2.0000e-03$	$8.0241e-04$	$2.5652e-04$
	1.3934	1.2186	1.3449	1.6453	
2^{-24}	$1.4600e-03$	$5.6000e-03$	$2.4000e-03$	$9.7847e-04$	$3.2349e-04$
	1.3731	1.2492	1.2745	1.5968	
2^{-27}	$1.6600e-03$	$6.4000e-03$	$2.7000e-03$	$1.2000e-03$	$3.9531e-04$
	1.3648	1.2618	1.2152	1.5495	
2^{-30}	$1.8400e-03$	$7.2000e-03$	$3.0000e-03$	$1.3000e-03$	$4.7123e-04$
	1.3617	1.2538	1.1680	1.5035	
$d^{\mathcal{N},\mathcal{M}}$	$1.8400e-03$	$7.2000e-03$	$3.0000e-03$	$1.3000e-03$	$4.7123e-04$
$p_{uni}^{\mathcal{N},\mathcal{M}}$	1.3617	1.2538	1.1680	1.5035	

Table 2: *Maximum point-wise errors and the corresponding order of convergence for Example 1 on a modified graded mesh using scheme* (15)

	Number of Intervals $\mathcal{N}, \mathcal{M}$				
	$\mathcal{N} = 84$	$\mathcal{N} = 168$	$\mathcal{N} = 336$	$\mathcal{N} = 672$	$\mathcal{N} = 1344$
ε	$\mathcal{M} = 5$	$\mathcal{M} = 20$	$\mathcal{M} = 80$	$\mathcal{M} = 320$	$\mathcal{M} = 1280$
2^{-3}	$9.4000e-03$	$2.7000e-03$	$7.0292e-04$	$1.8291e-04$	$4.9051e-05$
	1.8112	1.9293	1.9422	1.8988	
2^{-6}	$1.1100e-03$	$3.5000e-03$	$9.9420e-04$	$2.7750e-04$	$8.2428e-05$
	1.6599	1.8145	1.8411	1.7513	
2^{-9}	$1.1300e-03$	$3.7000e-03$	$1.1000e-03$	$3.2987e-04$	$1.0683e-04$
	1.6180	1.7392	1.7442	1.6266	
2^{-12}	$1.1300e-03$	$3.7000e-03$	$1.1000e-03$	$3.5990e-04$	$1.2389e-04$
	1.6181	1.6834	1.6735	1.5385	
2^{-15}	$1.1300e-03$	$4.3000e-03$	$1.6000e-03$	$4.7883e-04$	$1.3894e-04$
	1.6119	1.4536	1.6975	1.7850	
2^{-18}	$1.1900e-03$	$5.2000e-03$	$2.1000e-03$	$6.6140e-04$	$1.8765e-04$
	1.7785	1.6518	1.6354	1.8175	
2^{-21}	$1.3100e-03$	$6.1000e-03$	$2.6000e-03$	$8.6310e-04$	$2.5027e-04$
	1.8940	1.6578	1.5750	1.7861	
2^{-24}	$1.4200e-03$	$7.0000e-03$	$3.1000e-03$	$1.1000e-03$	$3.2024e-04$
	1.6196	1.7805	1.5176	1.7547	
2^{-27}	$1.5200e-03$	$7.8000e-03$	$3.6000e-03$	$1.3000e-03$	$3.9701e-04$
	1.9542	1.6154	1.7623	1.7233	
2^{-30}	$1.6000e-03$	$8.6000e-03$	$4.1000e-03$	$1.6000e-03$	$4.8006e-04$
	1.9022	1.5571	1.6089	1.6922	
$d^{\mathcal{N},\mathcal{M}}$	$1.6000e-03$	$8.6000e-03$	$4.1000e-03$	$1.6000e-03$	$4.8006e-04$
$p_{uni}^{\mathcal{N},\mathcal{M}}$	1.9022	1.5571	1.6089	1.6922	

Table 3: *Maximum point-wise errors and the corresponding order of convergence for Example 2 on a modified graded mesh using scheme* (13)

ε	Number of Intervals $\mathcal{N}, \mathcal{M}$				
	$\mathcal{N} = 84$ $\mathcal{M} = 5$	$\mathcal{N} = 168$ $\mathcal{M} = 20$	$\mathcal{N} = 336$ $\mathcal{M} = 80$	$\mathcal{N} = 672$ $\mathcal{M} = 320$	$\mathcal{N} = 1344$ $\mathcal{M} = 1280$
2^{-3}	$1.0565e-04$	$3.0122e-05$	$8.3177e-06$	$2.3937e-06$	$7.6229e-07$
	1.8104	1.8565	1.7970	1.6508	
2^{-6}	$1.5408e-04$	$5.3824e-05$	$1.6708e-05$	$5.2492e-06$	$1.8022e-06$
	1.5173	1.6877	1.6704	1.5424	
2^{-9}	$1.6659e-04$	$6.3801e-05$	$2.1436e-05$	$7.2210e-06$	$2.6525e-06$
	1.3846	1.5735	1.5698	1.4448	
2^{-12}	$1.6920e-04$	$6.6955e-05$	$2.3753e-05$	$8.4545e-06$	$3.2711e-06$
	1.3375	1.4951	1.4903	1.3699	
2^{-15}	$1.7144e-04$	$6.8827e-05$	$2.5610e-05$	$9.5467e-06$	$3.8417e-06$
	1.3166	1.4263	1.4236	1.3133	
2^{-18}	$1.8052e-04$	$7.0612e-05$	$2.7351e-05$	$1.0617e-05$	$4.4059e-06$
	1.3542	1.3683	1.3651	1.2689	
2^{-21}	$2.0035e-04$	$7.5085e-05$	$2.9004e-05$	$1.1683e-05$	$4.9695e-06$
	1.4160	1.3723	1.3118	1.2332	
2^{-24}	$2.3038e-04$	$9.8989e-05$	$3.0620e-05$	$1.2744e-05$	$5.5335e-06$
	1.2187	1.6928	1.2646	1.2036	
2^{-27}	$2.7570e-04$	$1.2149e-04$	$3.2179e-05$	$1.3797e-05$	$6.0980e-06$
	1.1822	1.9167	1.2217	1.1780	
2^{-30}	$3.1311e-04$	$1.4101e-04$	$3.7471e-05$	$1.4841e-05$	$6.6619e-06$
	1.1509	1.9119	1.3362	1.1556	
$d^{\mathcal{N},\mathcal{M}}$	$3.1311e-04$	$1.4101e-04$	$3.7471e-05$	$1.4841e-05$	$6.6619e-06$
$p_{uni}^{\mathcal{N},\mathcal{M}}$	1.1509	1.9119	1.3362	1.1556	

Table 4: *Maximum point-wise errors and the corresponding order of convergence for Example 2 on a modified graded mesh using scheme* (15)
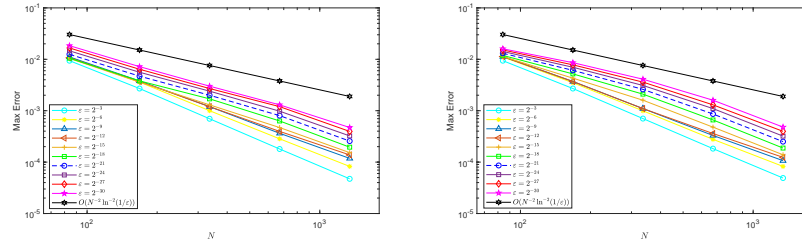
ε	Number of Intervals $\mathcal{N}, \mathcal{M}$				
	$\mathcal{N} = 84$ $\mathcal{M} = 5$	$\mathcal{N} = 168$ $\mathcal{M} = 20$	$\mathcal{N} = 336$ $\mathcal{M} = 80$	$\mathcal{N} = 672$ $\mathcal{M} = 320$	$\mathcal{N} = 1344$ $\mathcal{M} = 1280$
2^{-3}	$1.0178e-04$	$2.9341e-05$	$8.0678e-06$	$2.2905e-06$	$7.0284e-07$
	1.7945	1.8626	1.8165	1.7044	
2^{-6}	$1.2021e-04$	$3.9857e-05$	$1.1346e-05$	$3.1890e-06$	$9.6295e-07$
	1.5926	1.8127	1.8310	1.7276	
2^{-9}	$1.1696e-04$	$4.1225e-05$	$1.2193e-05$	$3.5503e-06$	$1.1220e-06$
	1.5044	1.7575	1.7801	1.6619	
2^{-12}	$1.1120e-04$	$4.0477e-05$	$1.2584e-05$	$3.8367e-06$	$1.2732e-06$
	1.4580	1.6856	1.7136	1.5913	
2^{-15}	$1.1026e-04$	$3.9240e-05$	$1.2814e-05$	$4.1096e-06$	$1.4249e-06$
	1.4906	1.6146	1.6407	1.5281	
2^{-18}	$1.1865e-04$	$5.6710e-05$	$1.2882e-05$	$4.3681e-06$	$1.5760e-06$
	1.7650	2.1382	1.5603	1.7708	
2^{-21}	$1.4002e-04$	$7.2639e-05$	$1.7165e-05$	$4.6091e-06$	$1.7255e-06$
	1.9468	2.0813	1.8969	1.4175	
2^{-24}	$1.7524e-04$	$8.5364e-05$	$2.4497e-05$	$4.8268e-06$	$1.8733e-06$
	1.8376	1.8010	2.3435	1.3655	
2^{-27}	$2.2202e-04$	$9.6868e-05$	$3.2831e-05$	$5.5598e-06$	$2.0192e-06$
	1.6966	1.5610	2.0620	1.7612	
2^{-30}	$2.7531e-04$	$1.0342e-04$	$4.1820e-05$	$7.3340e-06$	$2.1624e-06$
	1.8125	1.9063	2.0115	1.7619	
$d^{\mathcal{N},\mathcal{M}}$	$2.7531e-04$	$1.0342e-04$	$4.1820e-05$	$7.3340e-06$	$2.1624e-06$
$p_{uni}^{\mathcal{N},\mathcal{M}}$	1.8125	1.9063	2.0115	1.7619	

Table 5: *Comparison of maximum point-wise errors and the corresponding order of convergence for Example 1 on a modified graded mesh using scheme* (13)
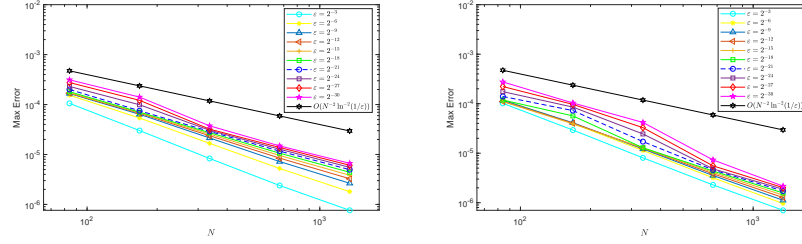
	HODIE scheme on modified graded mesh				
	$\mathscr{N} = 32$	$\mathscr{N} = 64$	$\mathscr{N} = 128$	$\mathscr{N} = 256$	$\mathscr{N} = 512$
ε	$\Delta t = 0.025$	$\Delta t = 0.025/4$	$\Delta t = 0.025/4^2$	$\Delta t = 0.025/4^3$	$\Delta t = 0.025/4^4$
2^{-6}	$8.999e-3$	$3.8000e-03$	$1.2000e-03$	$3.6372e-04$	$1.1823e-04$
	1.6443	1.6842	1.7058	1.6212	
2^{-8}	$9.322e-3$	$3.7000e-03$	$1.2000e-03$	$3.9593e-04$	$1.3800e-04$
	1.6221	1.6259	1.6130	1.5205	
2^{-10}	$1.0400e-03$	$3.6000e-03$	$1.3000e-03$	$4.7031e-04$	$1.5294e-04$
	1.5315	1.4188	1.5127	1.6206	
Result in [3]	On the Shishkin mesh				
2^{-6}	$8.998e-3$	$2.906e-3$	$1.033e-3$	$3.298e-4$	$1.032e-4$
	1.630	1.492	1.647	1.677	
2^{-8}	$9.322e-3$	$3.009e-3$	$9.817e-4$	$3.128e-4$	$1.059e-4$
	1.631	1.616	1.650	1.563	
2^{-10}	$9.411e-3$	$3.038e-3$	$9.961e-4$	$3.201e-4$	$1.007e-4$
	1.631	1.609	1.638	1.669	

Table 6: *Comparison of maximum point-wise errors and the corresponding order of convergence for Example 1 on a modified graded mesh using scheme* (15)

	Midpoint Scheme on Modified graded mesh				
	$\mathscr{N} = 32$	$\mathscr{N} = 64$	$\mathscr{N} = 128$	$\mathscr{N} = 256$	$\mathscr{N} = 512$
ε	$\Delta t = 0.025$	$\Delta t = 0.025/4$	$\Delta t = 0.025/4^2$	$\Delta t = 0.025/4^3$	$\Delta t = 0.025/4^4$
10^{-1}	$9.4000e-03$	$2.7000e-03$	$7.0292e-04$	$1.8291e-04$	$4.9051e-05$
	1.8112	1.9293	1.9422	1.8988	
10^{-2}	$1.1100e-03$	$3.5000e-03$	$9.9420e-04$	$2.7750e-04$	$8.2428e-05$
	1.6599	1.8145	1.8411	1.7513	
10^{-3}	$1.1300e-03$	$3.7000e-03$	$1.1000e-03$	$3.2987e-04$	$1.0683e-04$
Result in [17]	On the Shishkin mesh				
10^{-1}	$2.3969e-3$	$8.6402e-4$	$3.5400e-4$	$1.5854e-47$	$7.4832e-5$
	1.4720	1.2873	1.1589	1.0831	
10^{-2}	$1.2246e-2$	$4.4419e-3$	$1.6249e-3$	$6.0951e-4$	$2.3759e-4$
	1.4631	1.4509	1.4146	1.3592	
10^{-3}	$1.1994e-2$	$4.3716e-3$	$1.6070e-3$	$6.0543e-4$	$2.3789e-4$
	1.4561	1.4438	1.4084	1.3477	

(a) Log-log plot of Example 1 using scheme (13)(b) Log-log plot of Example 1 using scheme (15)

(c) Log-log plot of Example 2 using scheme (13)(d) Log-log plot of Example 2 using scheme (15)

Figure 4: Log-log plot of Examples 1 and 2

6 Discussion and conclusions

In this article, for the first time, we propose a modified graded mesh for convection-diffusion problems that provides second-order uniform convergence with respect to the perturbation parameter. We have presented effective numerical approaches in this work that are based on a modified graded mesh. In this two schemes are discussed namely hybrid finite difference schemes (15) and HODIE finite difference schemes (13), on a modified graded mesh. Both the above schemes show identical convergence, which can be viewed from the theoretical and numerical results established in this work.

In order to verify the theoretical estimation established, we conduct numerical experiments for two test problems for various values of ε and step sizes N and M. In order to find maximum point-wise error and corresponding order of convergence, we double the number of mesh points in the spatial direction and quadruple the number of mesh points in the time direction and apply the schemes (15) and (13) on the modified graded mesh. Through this procedure, we get the second-order convergence. These can be observed from

the results presented in Tables 1–2 for Example 1 and Tables 3–4 for Example 2. From the above tables, it can be confirmed that overall second-order uniform convergence. Corresponding log-log plots are provided for Examples 1 and 2. Figure 4 shows the overall second-order of convergence for various values of ε for Examples 1) and 2 with the schemes (15) and (13) on modified graded mesh.

It has been shown theoretically that the proposed methods, namely the hybrid finite difference scheme and the HODIE finite difference scheme, are uniformly convergent with first-order accuracy in time and almost second-order accuracy in space. We have also provided numerical results in order to verify the theoretical conclusions. The uniform convergence of the proposed methods is shown by the numerical results obtained for two test problems. Though the proposed method provides second-order convergence in space, the overall convergence rate of the method is not improved due to the backward-Euler approach used for the temporal direction. The ability to build higher-order, more time-accurate numerical schemes using the current setting is a feasible extension that may be used to improve accuracy while reducing computing costs.

Data Availability: Enquiries about data availability should be directed to the authors

Conflict of interest: The authors declare that they have no conflict of interest.

Acknowledgements

References

[1] Cai, X. and Liu, F. *A Reynolds uniform scheme for singularly perturbed parabolic differential equation*, ANZIAM Journal, 47 (2005) C633–C648.

[2] Chi-kuang, W. *The finite element method of singular perturbation prob-*

lem, Appl. Math. Mech. 5(1) (1984) 1011–1018.

[3] Clavero, C., Gracia, J.L. and Jorge, J.C. *High-order numerical methods for one-dimensional parabolic singularly perturbed problems with regular layers*, Numer. Methods Partial Differ. Equ. 21(1) (2005) 149–169.

[4] Clavero, C., Jorge, J.C. and Lisbona, F. *Uniformly convergent schemes for singular perturbation problems combining alternating directions and exponential fitting techniques*, Adv. Comput. Methods Bound. Inter. Layers. (1993) 33–52.

[5] Clavero, C., Gracia, J.L. and Lisbona, F. *High order methods on Shishkin meshes for singular perturbation problems of convection–diffusion type*, Numer. Algorithms, 22(1) (1999) 73–97.

[6] Clavero, C., Gracia, J.L. and Stynes, M. *A simpler analysis of a hybrid numerical method for time-dependent convection–diffusion problems*, J. Comput. Appl. Math. 235(17) (2011) 5240–5248.

[7] Friedman, A. *Partial differential equations of parabolic type*, Courier Dover Publications, 2008.

[8] Izadi, M. and Yuzbasi, S. *A hybrid approximation scheme for 1-d singularly perturbed parabolic convection-diffusion problems*, Math. Commun. 27(1) (2022) 47–62.

[9] Kadalbajoo, M.K. and Yadaw, A.S. *Parameter-uniform finite element method for two-parameter singularly perturbed parabolic reaction-diffusion problems*, Int. J. Comput. Methods 9(04) (2012) 1250047.

[10] Kaushik, A., Kumar, V., Sharma, M. and Sharma, N. *A modified graded mesh and higher order finite element method for singularly perturbed reaction–diffusion problems*, Math. Comput. Simul. 185 (2021) 486–496.

[11] Kaushik, A., Kumar, V., Sharma, M. and Vashishth, A.K. *A higher order finite element method with modified graded mesh for singularly perturbed two-parameter problems*, Math. Methods Appl. Sci. 43(15) (2020) 8644–8656.

[12] Kellogg, R.B. and Tsan, A. *Analysis of some difference approximations for a singular perturbation problem without turning points*, Math. Comput. 32(144) (1978) 1025–1039.

[13] Kopteva, N., *Uniform pointwise convergence of difference schemes for convection-diffusion problems on layer-adapted meshes*, Comput. 66(2) (2001) 179–197.

[14] Kopteva, N.V., *On the convergence, uniform with respect to a small parameter, of a scheme with weights for a one-dimensional nonstationary convection-diffusion equation*, Zh. Vychisl. Mat. Mat. Fiz, 37 (1997) 1213–1220.

[15] Kumar, S. and Vigo-Aguiar, J. *A parameter-uniform grid equidistribution method for singularly perturbed degenerate parabolic convection–diffusion problems*, J. Comput. Appl. Math. 404 (2022) 113273.

[16] Linss, T. *Layer-adapted meshes and fem for time-dependent singularly perturbed reaction-diffusion problems*, Int. J. Comput. Sci. Math. 1(2-4) (2007) 259–270.

[17] K. Mukherjee and S. Natesan. *Parameter-uniform hybrid numerical scheme for time-dependent convection-dominated initial-boundary-value problems*, Comput., 84(3) (2009) 209–230.

[18] Mukherjee, K. and Natesan, S. *Richardson extrapolation technique for singularly perturbed parabolic convection–diffusion problems*, Comput., 92 (2011) 1–32.

[19] Roos, H.G., Stynes, M. and Tobiska, L. *Robust numerical methods for singularly perturbed differential equations: convection-diffusion-reaction and flow problems*, Springer Science & Business Media, volume 24, 2008.

[20] Stynes, M. and Roos, H.G., *The midpoint upwind scheme*, Appl. Numer. Math. 23(3) (1997) 361–374.

[21] Sun, G. and Stynes, M. *Finite-element methods for singularly perturbed high-order elliptic two-point boundary value problems. I: reaction-diffusion-type problems*, IMA J. Numer. Anal. 15(1) (1995) 117–139.

[22] Tian, S., Liu, X. and An, R., *A higher-order finite difference scheme for singularly perturbed parabolic problem*, Math. Probl. Eng. 2021 (2021) 1–11.

[23] Vulanovic, R. *Higher-order monotone schemes for a nonlinear singular perturbation problem*, ZAMM Z. fur Angew. Math. 68(5), (1988) T428–T430.

[24] Vulanović, R. and Nhan, T.A. *Robust hybrid schemes of higher order for singularly perturbed convection-diffusion problems*, Appl. Math. Comput. 386 (2020) 125495.

[25] Ng-Stynes, M.J., O'Riordan, E. and Stynes, M. *Numerical methods for time-dependent convection-diffusion equations*, J. Comput. Appl. Math. 21(3) (1988) 289–310.